CrossMark

Influence of short-term heat treatment on the microstructure and mechanical properties of EN AW-6060 T4 extrusion profiles: Part A

Hannes Fröck[1] · Matthias Graser[2] · Michael Reich[1] · Michael Lechner[2] ·
Marion Merklein[2] · Olaf Kessler[1,3]

Abstract Aluminium alloys are applied in various industrial fields and play an important role concerning weight reduction especially in the automotive industry. Because of their higher strength, age-hardening alloys are commonly preferred. However, the cold formability in comparison to other materials like mild steels is quite low and due to this, complex parts are hardly producible at higher temperatures. One possibility to improve the cold formability of aluminium alloys is the so called tailor heat treatment. In this approach, a short-term heat treatment is conducted to achieve a local softening of the material due to dissolution of strengthening clusters (retrogression). This effect is used to improve the material flow, relief critical forming zones and enhance the overall formability of the material. Afterwards, strength can be increased again by aging. However, up till now tailor heat treatment has mainly been used for aluminium sheet. Further, a holistic process understanding, taking into account all process parameters as well as a complete integration of microstructural findings is missing. Therefore, the dissolution and precipitation behaviour during heating of Tailor Heat Treated Profiles (THTP) from the aluminium alloy EN AW-6060 T4 is investigated. Heating curves from 20 to 600 °C with heating rates of 0.01 up to 5 K/s are recorded, using the differential scanning calorimetry (DSC). Based on the peak temperatures of one DSC-curve, tensile tests were carried out after a comparable heat treatment. It is shown, that the mechanical properties gained by the tensile test correlate with the microstructure results of the DSC measurements. The correlation of the microstructure and the mechanical properties enables the derivation of optimal parameters for the development of THTP through a local softening. In Part B the heat treatment parameter for the subsequent forming process as well as the evolution of the mechanical properties during natural aging after different short-term heat treatments are discussed.

Keywords Aluminium · EN AW-6060 · Tailor Heat Treated Profiles (THTP) · Differential scanning calorimetry (DSC) · Dissolution · Precipitation

✉ Hannes Fröck
Hannes.froeck@uni-rostock.de

Matthias Graser
Matthias.graser@fau.de

Michael Reich
Michael.reich@uni-rostock.de

Michael Lechner
michael.lechner@fau.de

Marion Merklein
marion.merklein@fau.de

Olaf Kessler
olaf.kessler@uni-rostock.de

[1] Faculty of Mechanical Engineering and Marine Technology, University of Rostock, Albert-Einstein-Str. 2, 18059 Rostock, Germany

[2] Institute of Manufacturing Technology, Friedrich-Alexander-Universität Erlangen-Nürnberg, Egerlandstraße 11-13, 91058 Erlangen, Germany

[3] Department Life, Light and Matter (Research Competence Centre CALOR), Faculty of Interdisciplinary Research, University of Rostock, Albert-Einstein-Str. 25, 18059 Rostock, Germany

1 Introduction

Lightweight structures made of aluminium alloys are used today in many different areas, such as automotive or airplane. Especially precipitation hardening aluminium

384

Prod. Eng. Res. Devel. (2016) 10:383–389

alloys, such as the Al–Mg–Si-alloys, are widely used for automotive applications. This is due to the good ratio of stiffness and strength to density, corrosion resistance and weldability. The consequent use of lightweight structures leads to a reduction of vehicle weight, and therefore to a reduction of fuel consumption. Precipitation hardening aluminium profiles provide the possibility to produce light and rigid structures, such as are required in the automotive industry. In comparison to conventional profile materials such as steel, aluminum profiles have a reduced formability and tend to unacceptable cross-sectional deformations during the bending process of small radii. To improve the formability of aluminum profiles, a local short-term heat treatment has been established, to achieve a local softening of the material due to a dissolution of precipitations [1].

2 Thermal analysis by differential scanning calorimetry

2.1 Analysed aluminium and used DSC-devices

During short-term heat treatment of age-hardening aluminium alloys, such as Al–Mg–Si alloys, precipitation and dissolution reactions occur. To optimize the short-term heat treatment parameters, like the heating-rate, the maximum temperature and the cooling-rate, the knowledge of precipitation and dissolution behaviour is significantly important. The differential scanning calorimetry (DSC) is a suitable technique to record the precipitation and dissolution behaviour in situ during the heat treatment of aluminium alloys [2].

In the present study, the precipitation and dissolution behaviour of a hollow quadratic extrusion profile (20 mm × 20 mm × 2 mm) from the aluminium alloy EN AW-6060 T4 was investigated in a wide dynamic range. Heating curves from 20 to 600 °C with heating rates of 0.01 up to 5 K/s are recorded, using the DSC. The chemical composition of the analysed alloy is given in Table 1.

The heating experiments are performed in two different devices with different heating rates. For the slow rates between 0.01 and 0.1 K/s a heat-flux DSC (Sensys evo DSC, Setaram Instumentation) of the Calvet-type was utilized. The faster heating rates between 0.3 and 5 K/s are performed in a power-compensated DSC (PerkinElmer Pyris Diamond DSC, Perkin Elmer). For the measurements

in the Sensys evo DSC stacked samples were used. Each sample consists of 5 single discs with the dimension of Ø 6.0 mm × 2 mm. The mass of each stacked sample is about 752 mg. The sample is covered by one standard aluminium crucible and is capped with an aluminium lid. Substantial investigations of stacked samples were performed by Osten et al. The studies have shown that stacked samples and conventional bulk samples yield the same results in the thermal analysis using the DSC [3]. The samples for the measurements in the PerkinElmer Pyris Diamond have a cylindrical geometry with the dimensions of Ø 6.4 mm × 1 mm. The mass of each sample is about 82 mg. All samples were milled out of the profile. As reference material for all measurements, a 99.9995 % pure aluminium with the same geometry and mass was used.

2.2 Evaluation of raw data

It is necessary to eliminate a device-specific curvature of the raw measurement data to obtain evaluable DSC curves. In order to eliminate the device-specific curvature, a baseline measurement with two high-purity aluminium reference samples, has been performed directly before or after an alloy sample measurement. Every alloyed sample is scanned against a high-purity aluminium sample, whereas at the baseline measurement two high-purity aluminium samples are used. By subtracting the baseline from the sample measurement, the device-specific curvature can be removed from the raw measurement data [4].

For every heating rate in the Sensys evo DSC, four sample measurements were performed and for every heating rate in the PerkinElmer Pyris Diamond, six sample measurements were conducted. To compare the recorded data with different heating rates (β) and different sample masses (m_s), it is necessary to normalize the measured heat flow to the excess specific heat capacity [5].

$$C_{p_{excess}} = \frac{\dot{Q}_S - \dot{Q}_{BL}}{m_S \cdot \beta} \ in \ Jg^{-1}K^{-1} \tag{1}$$

$C_{p_{excess}}$: excess specific heat capacity; $\dot{Q}_S$: sample heat flow; $\dot{Q}_{BL}$: Baseline heat flow; m_S: sample mass; β: scan rate.

The maximum temperature was chosen with 600 °C for all heating rates such that all reactions have been finished before the maximum temperature has been reached. Thus, there are reaction-free areas at high and low temperatures. A perfect symmetry in the two DSC furnaces cannot be

Table 1 Mass fraction of alloying elements of the investigated material in %	Aluminium	Mass fraction in %							
	Alloy	Si	Fe	Cu	Mn	Mg	Cr	Zn	Ti
	EN AW-6060 T4	0.399	0.223	0.074	0.139	0.561	0.022	0.017	0.016
	DIN EN 573-3	0.3–0.6	0.1–0.3	≤0.1	≤0.1	0.35–0.6	≤0.05	≤0.15	≤0.1

achieved, so that a slight curvature of the measurement data exists after baseline subtraction. This curvature can be manually removed by the subtraction of a polynomial 3rd straight. The polynomial is thereby applied to the reaction-free areas at high and low temperatures. A detailed description of the evaluation of DSC heating curves gives Osten et al. [3]. In the present study, the identical evaluation of the raw measurement data was applied.

2.3 Peak assignment

Figure 1 shows an example of a DSC heating curve of the alloy EN AW-6060 T4, recorded with a heating rate of 0.03 K/s from 20 to 600 °C. It can be seen that exothermic and endothermic reactions alternate. A dissolution reaction occurs endothermic, precipitation reactions proceed exothermic. Accordingly in the shown DSC heating curves endothermic dissolution reactions appear as an exceeding deviation from the zero level. Exothermic precipitation reactions appear, however by a deviation below the zero level (see Fig. 1). In all shown DSC-curves, the zero level is displayed by a straight dotted line.

Due to the superimposition of the individual reactions, the interpretation of the heating curve is not always clear and may lead to misinterpretations.

In recent years, the precipitation and dissolution behaviour of Al–Mg–Si aluminium alloys in different initial conditions has been extensively studied [3], such that the individual peaks of the DSC heating curves can be assigned, through literature, to different reactions [6].

The excess specific heat capacity curve starts with a small exothermic peak (a). This peak is generally interpreted as a formation of clusters. These clusters can be formed due to a remaining potential of free alloying element atoms [7].

Afterwards an endothermic peak (B) is shown which is caused by the dissolution of clusters and GP-zones, which

have formed during the natural aging [8]. At some heating rates, the peak (B) is shaped as a two-step shoulder peak, indicating the overlapping of two dissolution reactions, (see Fig. 3, 0.1 K/s and 0.3 K/s).

The exothermic peaks (c) and (d) are widely interpreted as the formation of the metastable phases ß″ and ß′ [9]. With an increasing heating rate, the overlapping of these two peaks enlarge, so that the reactions at higher heating rates cannot be separated, and appear as one common peak (see Fig. 3). The endothermic peak (E) is the dissolution of the previously formed metastable phases ß″ and ß′ [10].

Following the precipitation and dissolution sequence the exothermic Peak (f) can be interpreted as the formation of equilibrium phase ß (Mg_2Si) [11]. With an increasing heating rate (see Fig. 3) the Peak (f) occurs only as a local minimum. This indicates that the overlapping of the reactions enlarges with an increasing heating rate and the interpretation of the DSC heating curves becomes more difficult. Hence the analysis of slow heating rates is essential for the comprehensive understanding of the proceeding reactions in addition to the recording of fast heating rates.

The endothermic Peak (G) at high temperatures represents the dissolution of equilibrium phase ß (Mg_2Si), and all other phases, which haven't been dissolved completely before. At a very low heating rate (see Fig. 3, 0.01 K/s) peak (G) is again shaped as an overlapping of two single endothermic dissolution peaks. [12].

At temperatures higher than 550 °C no additional reactions occur so that all alloying element atoms are solute in the aluminium.

Figure 2 shows the discussed DSC heating curve of EN AW-6060 T4, recorded with a heating rate of 0.03 K/s from 20 to 600 °C with all assigned reactions to the corresponding recorded peaks.
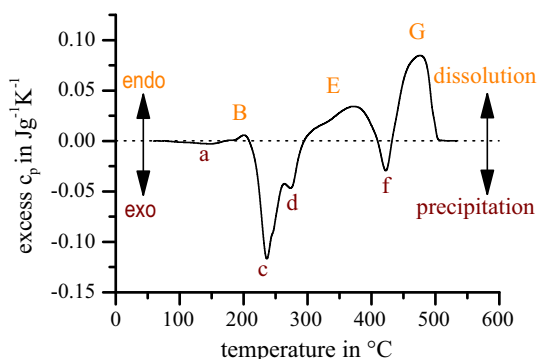

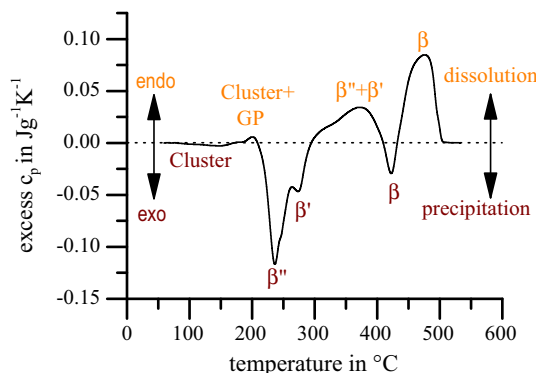**Fig. 1** Continuous heating DSC curve at 0.03 K/s of EN AW-6060 T4

Fig. 2 Continuous heating DSC curve at 0.03 K/s of EN AW-6060 T4 with all discussed possible reactions

386

Prod. Eng. Res. Devel. (2016) 10:383–389

2.4 Precipitation and dissolution behaviour of EN AW-6060 T4 in a wide dynamic range

Figure 3 shows selected excess specific heat capacity from heating curves of the alloy EN AW-6060 T4. The different DSC heating curves are arranged from a slow heating rate at the top of the diagram to a fast heating rate at the bottom. Every single curve is plotted with its own zero level which is displayed by a straight dotted line.

It is shown that the peak temperatures generally shift to higher temperatures with an increasing heating rate. The most obvious example of this evolution is the exothermic peak (c). At the heating rate of 0.01 K/s the peak temperature is about 220 °C and increases with a raising heating rate continuously to 360 °C at 5 K/s. Most of the other peak temperatures have a similar course.

Comparing the endothermic dissolution peak (B) and the exothermic precipitation peaks (c) and (d) it can be seen that with an increasing heating rate the formation of precipitation is more suppressed than the dissolution of precipitates. This development has been observed already on other aluminium alloys [3]. The formation and dissolution of precipitates are diffusion-controlled reactions. Hence, it is probable that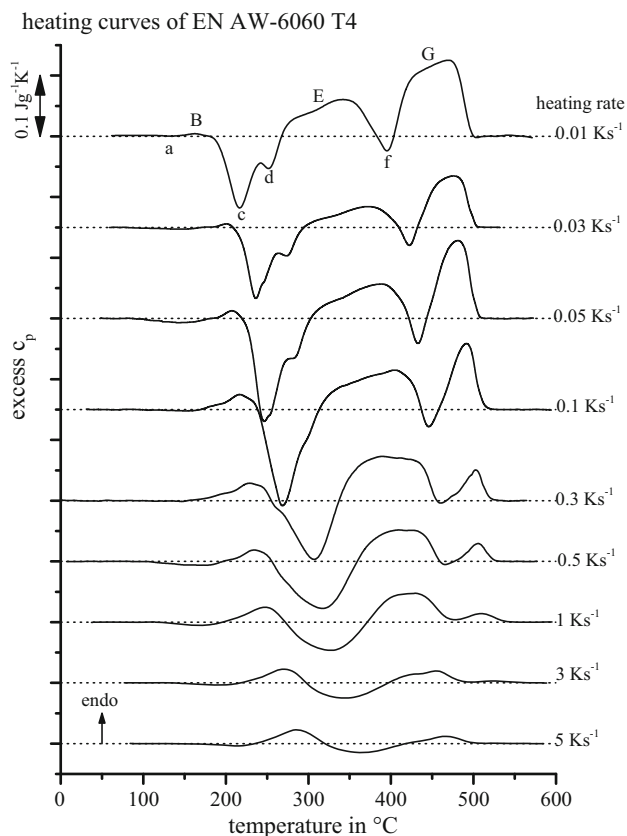 both reactions are progressively suppressed with an increasing heating rate. The necessary diffusion paths of the alloying element atoms to form a precipitate are much longer than the local diffusion paths of the dissolution of a precipitation, so it is conceivable that the precipitation kinetics is slower than the kinetics of dissolution, and therefore, the precipitation reactions are earlier suppressed than the dissolution reactions.

The reactions influence each other very significantly. One example of this dependence is the reaction (E). If the reactions (c) and (d) are increasingly suppressed at high heating rates, the following peak (E) becomes smaller, because if during the reactions (c) and (d) less precipitations are formed, less precipitations have to be dissolved in the subsequent reaction (E). The same shall apply for the peaks (f) and (G).

3 Correlation between thermal analysis and thermo-mechanical analysis

It is particularly important to know which effect a precipitation or dissolution reaction has on the mechanical properties of an alloy. Studies have already been conducted, to correlate a DSC heating curve with the related mechanical properties [13].

In order to determine the effect of precipitates, and dissolution reactions on the mechanical properties a heat treatment on the basis of DSC-Data has been performed. The analysed heating rate of 1 K/s displays the main precipitation and dissolution reactions. Out of the DSC heating curve, characteristic temperatures like peak temperatures and zero crossings were derived, as shown in Fig. 4.

According to these characteristic temperatures thermomechanical analyses were performed in the quenching and deformation dilatometer type Bähr 805 A/D, which unites the properties of a quenching dilatometer and a mechanical testing machine [14]. Further, the transferability of these results to macro-mechanical results has been proven by
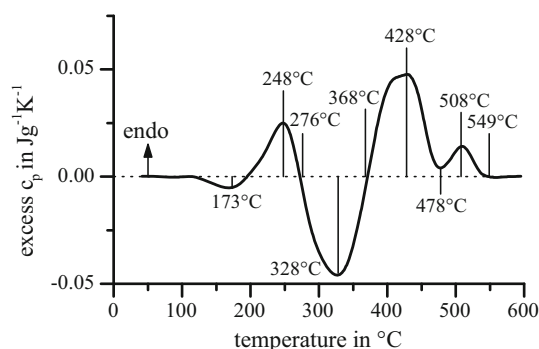

Fig. 3 Selected heating curves of EN AW-6060 T4

Fig. 4 Continuous heating DSC curve at 1 K/s of EN AW-6060 T4 with characteristic temperatures

Prod. Eng. Res. Devel. (2016) 10:383–389

387

uniaxial tensile tests according to the testing and documentation guideline for mechanical properties of aluminium materials in the automotive industry [15].

3.1 Tensile tests in deformation dilatometer

Tensile tests were performed after heating the samples with 1 K/s to the derived different characteristic temperatures. After reaching the peak temperature, the sample was quenched overcritically to room temperature. Immediately the tensile tests were carried out at room temperature in the same device. The tensile speed amounts 0.1 mm/s. All sets of parameters were performed for three times. The schematic measurement plan and sample geometry are shown in Fig. 5.

The samples used for the tensile test are specially adapted to the deformation dilatometer [16] and thus are not conform to the standard for tensile specimens. The flat samples have a gauge length of 10 mm and a cross-section of 8 mm^2. The change in length of the sample is measured tactile via transmission rods during the tensile test. The samples are heated inductively by a surrounding induction coil in an inert nitrogen atmosphere. An additional inner coil is perforated which can be used for gas quenching. Nitrogen was used as quenching medium for these tests. The temperature of the sample is controlled with thermocouples spot-welded on the specimen surface outside of the gauge length. The maximum temperature in the gauge length during welding of the thermocouple is below the temperature of the first reaction (a) which occurs in the thermal analysis. Combined with the short period of time, a thermal-induced change of the interested area of the sample during welding may be almost excluded.

Figures 6 and 7 display the continuous heating DSC curve at a heating rate of 1 K/s of EN AW-6060 T4 and the corresponding yield strength curve (Fig. 6) and tensile strength curve (Fig. 7). The error bars indicate the highest respectively the lowest recorded value of the parameter set. In general, the curves of yield strength and
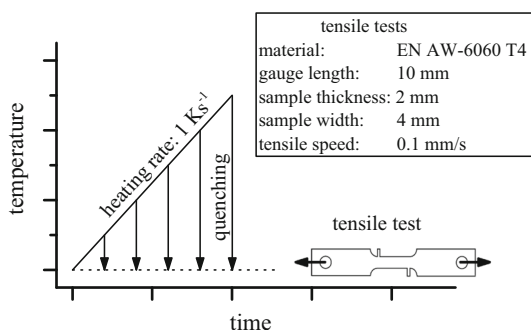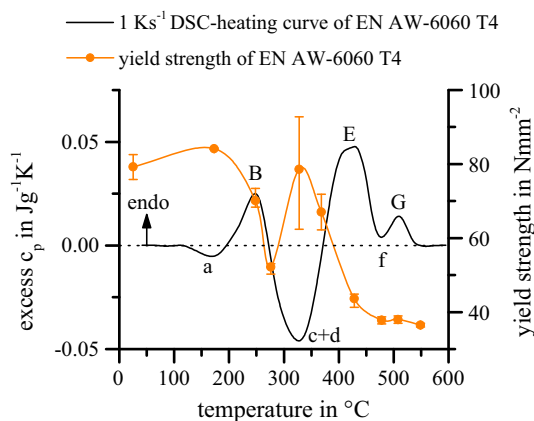

Fig. 6 Continuous heating DSC curve at 1 K/s of EN AW-6060 T4 correlated with the yield strength after an interrupted heat treatment
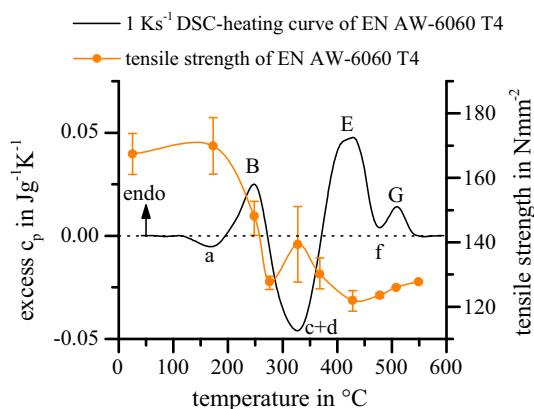

Fig. 7 Continuous heating DSC curve at 1 K/s of EN AW-6060 T4 correlated with the tensile strength after an interrupted heat treatment

tensile strength are quite similar, therefore, they will be discussed together.

In the initial state T4 the yield strength is around 80 N/mm^2 and tensile strength is around 170 N/mm^2. These values are in the normal range for the alloy EN AW-6060 T4 [17]. After heating the sample with 1 K/s to 173 °C the yield strength and the tensile strength rise slightly. The yield strength increases about 6 % and the tensile strength rises about 1.5 % This behaviour correlates with the first exothermic peak (a) of the DSC heating curve, and the related additional precipitation of clusters [18].

A further increase in the maximum temperature in the region of the endothermic dissolution peak (B), leads to a sharp reduction of the yield and tensile strength. As discussed previously, the peak (B) indicates the dissolution of GP-zones. The GP-zones formed during the natural aging cause a strong increase in strength [19]. Hence the strength of the alloy has to decrease significantly with the dissolution of GP-zones, which is also reflected in the curves.

Fig. 5 Schematic measurement plan of the thermo-mechanical analysis

388

Prod. Eng. Res. Devel. (2016) 10:383–389

Compared to the initial state, the yield strength decreases around 35 % and the tensile strength decreases about 25 % during the heat treatment up to 276 °C.

Increasing the maximum temperature to 328 °C the area of the exothermic precipitation peak (c) + (d) is achieved. The precipitation of the ß″-phase causes a substantial increase in strength [20]. The ß″-phase transforms to the ß′-phase by higher temperatures or longer periods and leads to a lower increase of the strength, than the ß″-phase [18]. Due to the precipitation of these phases there is an increase in strength. Compared to the strength at 276 °C, the yield strength rises about 50 % and the tensile strength rises around 9 %. Due to the wide overlap of the two precipitation reactions even small temperature differences cause varying proportions of ß″ and ß′-phases, leading to different mechanical properties, as read on the error bar at this temperature.

A further increase of the maximum temperature during the heat treatment leads to a dissolution of these precipitates and thus to a softening of the material, as is apparent at temperatures above 400 °C. For a verification of the transferability of the results of the DSC-tests and quenching and deformation dilatometry additional standard uniaxial tensile tests were conducted.

3.2 Uniaxial tensile tests after heat treatment

The tensile specimens for these tests are initially laser cutted from the extrusion profiles with a material allowance of 1 mm in the area of the test length by a Trumpf CO_2-Laser and subsequently milled to their final dimensions. The standard specimen dimensions for a measuring length of 50 mm according to DIN 50125 are scaled with a factor of 0.7 to fit the profile geometry (see Fig. 8).

Due to efforts using the THTP approach in industrial applications the tests were conducted according to the testing and documentation guideline for mechanical properties of aluminum materials in the automotive industry (PuD-Al). This guideline prescribes a stress-controlled elongation in the area of the yield strength identification with 5 MPa/s and afterwards a strain-controlled elongation with 0.667 %/s. The machine used for testing is a universal testing machine Zwick 100 with subjoined tactile length and width sensors.
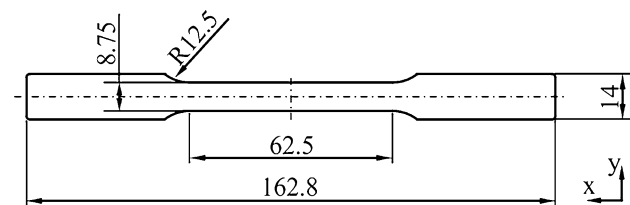
For the heat treatment of the specimens a convection chamber furnace N120/85 HA with a volume of 120 l and maximum temperature of 850 °C has been used. The heating is done from all side walls and is distributed by a horizontal convection. This leads to temperature homogeneity of $\Delta T = 8$ °C according to DIN 17052-1. The oven was used to heat the specimens with an initial rate of 2 K/s which decreased slightly to 0.5 K/s at higher temperatures (Fig. 9). Therefore the results can be correlated with DSC heating rates of 1 K/s. After the desired temperature was reached the specimens were removed from the oven, quenched overcritically in water and tested subsequently.

The results of the uniaxial tensile test for slow heating of the specimens combined with a subsequent fast quenching are depicted in Fig. 10 regarding the yield strength, tensile strength and uniform elongation. Heat treatment temperatures from 200 to 250 °C result in a decrease of all mechanical properties, because the MgSi-clusters are dissolved in the aluminium matrix. The yield strength decreases from 82 MPa in T4 condition to 64 MPa after a heat treatment of 275 °C, the tensile strength decreases from 173 MPa to 146 MPa and the uniform elongation from 17.2 to 11.6 %. For 275 °C there is still a decrease of the strength values, however, the uniform elongation shows a converse behaviour and increases to 16.8 %. Subsequently, for higher temperatures the uniform elongation decreases once again and reaches a value of 14.4 % at 400 °C. The yield and tensile strength increase after heat treatments at 300 and 325 °C and reach values of 70 and 140 MPa respectively. The increase of strength values as well as the decrease of the uniform elongation are ascribed to the β″ and β′-precipitations. Those precipitates not only oppose the softening due to the MgSi-clusters' dissolution but also lead to lower ductility of the material [21]. At 400 °C the tensile strength as well as the yield strength reach their minimum values with 49 and 128 MPa.

The results of the two performed series of tensile tests provide a very high level of agreement in the course of the mechanical properties (see Fig. 10). Slight deviations in the absolute values can be attributed to the different used tensile specimen geometries and to the marginal differences during the two performed heat treatments.
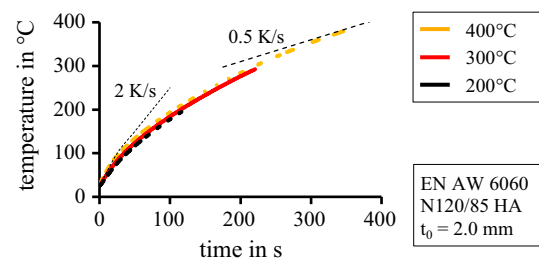
Fig. 8 Tensile and bending specimen

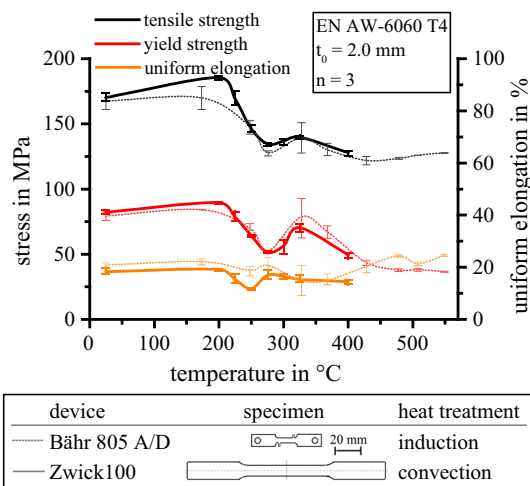**Fig. 9** Heating curves–convection chamber oven

Fig. 10 Mechanical properties (yield strength, tensile strength and uniform elongation)—macroscopic tensile tests compared to deformation dilatometry

4 Conclusion

The results demonstrate that it is possible to in situ analyse dissolution and precipitation reactions during retrogression annealing of tailor heat-treated aluminium profiles by DSC tests. The DSC results well correlated with microstructure changes and mechanical properties. For the tensile tests in the deformation dilatometer as well as by a standard universal testing machine the values of the yield and tensile strength agreed with each other.

For a successful transfer of knowledge gained from these short-term heat treatment investigations the heating rate has to be further increased, to reduce process durations. Therefore in Part B [22] of these investigations the influence of a short-term heat treatment by laser irradiation will be investigated in dependence of the heat treatment temperature. Thereon recommendations for a purposeful choice of heat treatment temperatures of Tailor Heat Treated Profiles will be submitted.

References

1. Merklein M, Böhm W, Lechner M (2012) Tailoring material properties of aluminum by local laser heat treatment. Phys Procedia 39:232–239
2. Milkereit B, Osten J, Schick C et al (2012) Continuous heating dissolution diagrams of aluminum alloys. In: Weiland H, Rollett AD, Cassada WA (eds) Proceedings 13th international conference on aluminum alloys. Wiley, Hoboken, pp 1095–1100
3. Osten J, Milkereit B, Schick C, Kessler O (2015) Dissolution and precipitation behaviour during continuous heating of Al–Mg–Si alloys in a wide range of heating rates. Materials 8:2830–2848
4. Milkereit B, Kessler O, Schick C (2009) Recording of continuous cooling precipitation diagrams of aluminium alloys. Thermochim. Acta 492(Special Issue: Calorimetry on a Nanoscale):73–78
5. Höhne G, Hemminger W, Flammersheim H (2003) Differential scanning calorimetry: an introduction for practitioners, 2nd rev. and enl. ed, Springer, Berlin
6. Takeda M, Ohkubo F, Shirai T et al (1996) Precipitation behaviour of Al–Mg–Si ternary alloys. Mater Sci Forum 217–222:815–820
7. Kim SN, Kim JH, Tezuka H et al (2013) Formation behavior of nanoclusters in Al–Mg–Si alloys with different Mg and Si concentration. Mater Trans 54(03):297–303
8. Murayama M, Hono K (1999) Pre-precipitate clusters and precipitation processes in Al–Mg–Si alloys. Acta Mater 47(5):1537–1548
9. Tsao CS, Chen CY, Jeng US et al (2006) Precipitation kinetics and transformation of metastable phases in Al–Mg–Si alloys. Acta Mater 54(17):4621–4631
10. Edwards GA, Stiller K, Dunlop GL et al (1998) The precipitation sequence in Al-Mg–Si alloys. Acta Mater 46(11):3893–3904
11. Doan LC, Ohmori Y, Nakai K (2000) Precipitation and dissolution reactions in a 6061 aluminum alloy. Mater Trans 41(2):300–305
12. Gupta AK, Lloyd DJ (1999) Study of precipitation kinetics in a super purity Al-0.8 pct Mg-0.9 pct Si alloy using differential scanning calorimetry. Metall and Mat Trans A 30(3):879–884
13. Miao WF, Laughlin DE (2000) A differential scanning calorimetry study of aluminum alloy 6111 with different preaging treatments. J Mater Sci Lett 19(3):201–203
14. Reich M, Keßler O (2012) Quenching simulation of aluminum alloys including mechanical properties of the undercooled states. Mater Perform Charact 1(1):104632
15. PuD (2005) Prüf- und Dokumentationsrichtlinie für die mechanischen Kennwerte von Walzprodukten aus Aluminium
16. Osten J, Söllig P, Reich M et al (2014) Softening of high-strength steel for laser assisted clinching. Adv Mater Res 966–967:617–627
17. DIN (2013) Aluminium und Aluminiumlegierungen—Stranggepresste Stangen, Rohre und Profile—Teil 2: Mechanische Eigenschaften (755-2)
18. Ostermann F (2014) Anwendungstechnologie aluminium, 3rd edn edn. Springer, Berlin
19. Kammer C (2011) Aluminium-Taschenbücher digital: Band 1–3 Gesamtversion, [2. bearb. Ausg.]. Alu Media GmbH, Düsseldorf
20. Marioara C, Andersen S, Jansen J et al (2003) The influence of temperature and storage time at RT on nucleation of the β″ phase in a 6082 Al–Mg–Si alloy. Acta Mater 51(3):789–796
21. Geiger M, Merklein M, Vogt U (2009) Aluminum tailored heat treated blanks. Prod Eng Res Devel 3(4–5):401–410
22. Graser M, Fröck H, Lechner M et al (2016) Influence of short-term heat treatment on the microstructure and mechanical properties of EN AW-6060 T4 extrusion profiles–Part B. Prod Eng Res Devel. doi:10.1007/s11740-016-0684-5